The Conformational Behaviour of Non-Hydrolizable Lactose Analogues: The Thioglycoside, Carbaglycoside, and Carba-Iminoglycoside Cases

Esther Montero,[a] Alicia García-Herrero,[a] Juan Luis Asensio,[a] Keisuke Hirai,[b] Seiichiro Ogawa,[b] Francisco Santoyo-González,[c] F. Javier Cañada,*[a] and Jesús Jiménez-Barbero*[a]

Keywords: Carbohydrates / Glycosides / Conformation analysis / Molecular modeling / Carbasugars

The conformational behaviours of several nonhydrolizable lactose analogues, namely methyl α-thiolactoside (**1**), methyl β-carbalactoside (**2**) and methyl β-carbaiminolactoside (**3**) have been studied using a combination of NMR spectroscopy (*J* and NOE data) and molecular mechanics calculations. Analogies and differences with the natural compounds have been found.

Introduction

In recent years the search for new glycosidase inhibitors and stable sugar mimetics has led to different groups of oligosaccharide analogues with the glycosidic oxygen substituted by heteroatoms.[1] Thus, *C*- and *S*-glycosides may serve as carbohydrate mimics resistant to metabolic processes.[2] On the same basis, carbasugars with the endocyclic oxygen substituted by carbon have also been prepared.[3] Nevertheless, for these pseudodisaccharides to be biologically useful, one of the requirements is that their conformational behaviour should be analogous to that of the natural compound, in order to minimize entropic costs of the recognition process with the receptor.[4] Therefore, it is important to determine how the synthetic derivatives are affected by such modifications. In this context, we have recently reported that thiocellobiose is bound by *Streptomyces Sp.* β-glucosidase in the conformation usually found for regular *O*-glycosides (*syn*-Φ,Ψ).[5] In contrast, we also have described that the *C*-glycosyl analogue of lactose is bound by *E. coli* β-galactosidase in an unusual high energy conformation.[6] These results have prompted us to extend our studies to determine which is the degree of similarity between oligosaccharides and other saccharide analogues.[7] It is obvious that the substitution of the exo- or endocyclic oxygens by other atoms will result in a change in both the size and the electronic properties of the glycosidic linkage, particularly in the anomeric effects.[8] In addition, for nitrogen-containing compounds, the characteristics of the nitrogen atom may also produce a pH-dependent conformational behaviour. The study of several thioglycosides[9] and carbasugars[10] would provide new insights on this topic since, due to the different contribution of stereoelectronic and steric effects, pseudoglycosidic bonds may be expected 1to be conformationally different to *O*-glycosidic linkages. In fact, the C−S bond length (1.78 Å) and C−S−C bond angle (99°) strongly differ from the values for C−O (1.41 Å) and C−O−C (116°). On the other hand, the C−N distance and C−N−C bond angle values are 1.47 Å and between 116.5−119.6°, according to MM3* calculations. On this basis, we report here the conformational study of the thioglycoside- (**1**), carbaglycoside-, (**2**) and carbaiminoglycoside (**3**) analogues of lactose (**4**), using a combination of NMR spectroscopy and MM3* molecular mechanics and dynamics calculations.[11] These lactose analogues have also been tested as *E. coli* β-galactosidase inhibitors.

Results and Discussion

Molecular Mechanics and Dynamics Calculations

The adiabatic surfaces calculated for **1**−**3** (Figure 1) using different force fields (AMBER*, MM2*, and MM3*).[12]

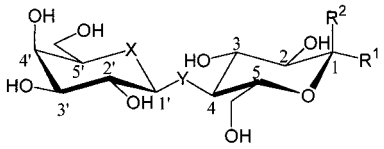

	X	Y	R^1	R^2
1	O	S	H	OMe
2	CH_2	O	OMe	H
3	CH_2	NH	OMe	H
4	O	O	OMe	H

Figure 1. Schematic representation of compounds **1**−**4**, showing the atomic numbering; for carbasugars, the $-CH_2-$ methylene carbon atom is named 5a-carbon; however, here we have used C-7 for sake of clarity and to be more readily understandable by the reader

[a] Instituto de Química Orgánica, CSIC,
Juan de la Cierva 3, 28006 Madrid, Spain
[b] Department of Applied Chemistry, Faculty of Science and Technology, Keio University,
3−14−1 Hiyoshi, Kohoku-ku, Yokohama 223−8522, Japan
[c] Facultad de Farmacia, Departamento de Química Farmaceútica, Universidad de Granada,
Spain

Supporting information for this article is available on the WWW under http://www.wiley-vch.de/home/eurjoc or from the author.

  1434−193X/00/0510−1945 $ 17.50+.50/0

From these energy surfaces, probability distributions were obtained according to a Boltzmann function. Glycosidic torsion angles are defined as Φ H1′−C1′-Y−C4 and Ψ C1′-Y−C4−H4. Three different conformational families are found in all cases (Table 1, Figure 2) and a fourth one is also found for carbaglycosides **2** and **3**.

The global minimum of **1** is located in the *syn*-Φ/*anti*-Ψ region and has dihedral angles of Φ = 38 ± 6 and Ψ = 173 ± 3, with populations between 50−62%. An additional local minimum (22−29%) is the *syn*-Φ/*syn*-Ψ conformer (Φ = 52 ± 3 and Ψ = −12 ± 4). These population values are in contrast with those predicted and experimentally proven for methyl α-lactoside,[13] for which there is a much higher contribution (>90%) of this *syn*-Φ/*syn*-Ψ conformation. A third conformational family (Figure 2, *anti*-Φ/*syn*-Ψ, Φ = 171 ± 3, Ψ = 2 ± 4) is also predicted to exist with 13−17% population. This conformation is below experimental detection for lactose derivatives, although it has been detected for the *C*-glycosyl analogue of lactose in solution (ca. 5%),[14,15] and, in fact, has been found in the molecular complex between *C*-lactose and *E. coli* β-galactosidase.[6]

Table 1. Torsional angle values (Φ,Ψ) of the predicted conformers A-D for the low energy minima and MM2*, AMBER (compound **1**), and MM3* (compounds **2** and **3**) populations; the regions around Φ extend ca. 20° and around Ψ ca. 30°; for compounds **1** and *O*-glycosyl[13] natural compound **4**, the range of populations predicted by AMBER and MM2* are given

Compound Conformer[a]	Torsion angle (Φ,Ψ)	Pop (%) AMBER MM2*	Compound Conformer[a]	Torsion angle (Φ,Ψ)	Pop (%) MM3* ε = 80	Compound Conformer[a]	Torsion angle (Φ,Ψ)	Pop (%) MM3* ε = 80
1-A	56/-9	22−29	2-A	53/32	52	3-A$^{\#2}$	46/21	83
1-B	33/172	50−62	2-B	38/180	<1	3-B$^{\#2}$	14/179	2
1-C	169/6	13−17	2-C	178/1	<1	3-C$^{\#2}$	176/-10	1
1-D	-	-	2-D	54/-54	48	3-D$^{\#2}$	9/-45	14
4-A	50/-1	75−95	3-A$^{\#1}$	53/32	84	3-A$^{\#3}$	54/0	48
4-B	21/174	5−15	3-B$^{\#1}$	38/180	12	3-B$^{\#3}$	18/180	2
4-C	170/4	0−15	3-C$^{\#1}$	178/1	<1	3-C$^{\#3}$	178/-5	<1
4-D	-	-	3-D$^{\#1}$	54/-54	4	3-D$^{\#3}$	-36/-36	50

[a] Conformers A−D: A *syn*-Φ/*syn*′-Ψ; B *syn*-Φ/*anti*-Ψ; C *anti*-Φ/*syn*-Ψ; D non-exo/*syn*-Ψ. For compound **3** $^{\#1}$ NH2, **3**$^{\#2}$ NH (pro*R*) **3**$^{\#3}$ NH (pro*S*).

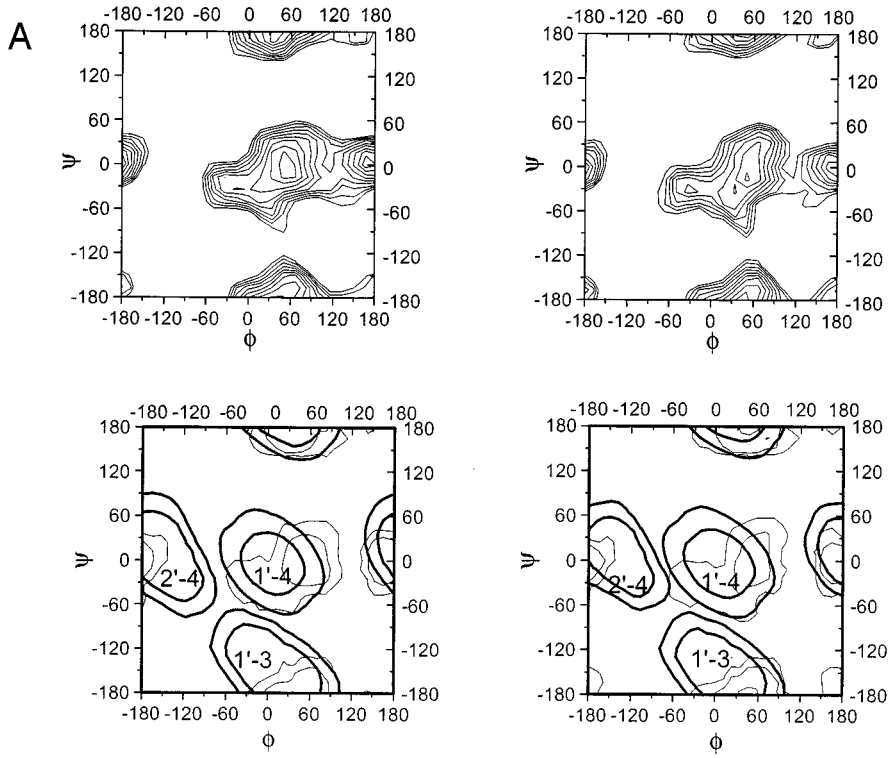

Figure 2. (A) Adiabatic (top) and population distribution (bottom) maps for compound **1**; MM2* maps are given on the left-hand side and AMBER* maps on the right-hand side; short exclusive inter-residue distances are also superimposed in the distribution maps; (B) Adiabatic (left) and population distribution (right) MM3* maps for compound **2**; (C) Adiabatic (left) and population distribution (right) MM3* maps for compound **3**$^{\#1}$**-NH$_2$**; (D) Adiabatic (left) and population distribution (right) MM3* maps for compound **3**$^{\#2}$**-NH**; (E) Adiabatic (left) and population distribution (right) MM3* maps for compound **3**$^{\#3}$**-NH**; in all cases, energy contours are given every 1.5 kcal/mol; distribution contours are given at 10%, 1% and 0.1% of population

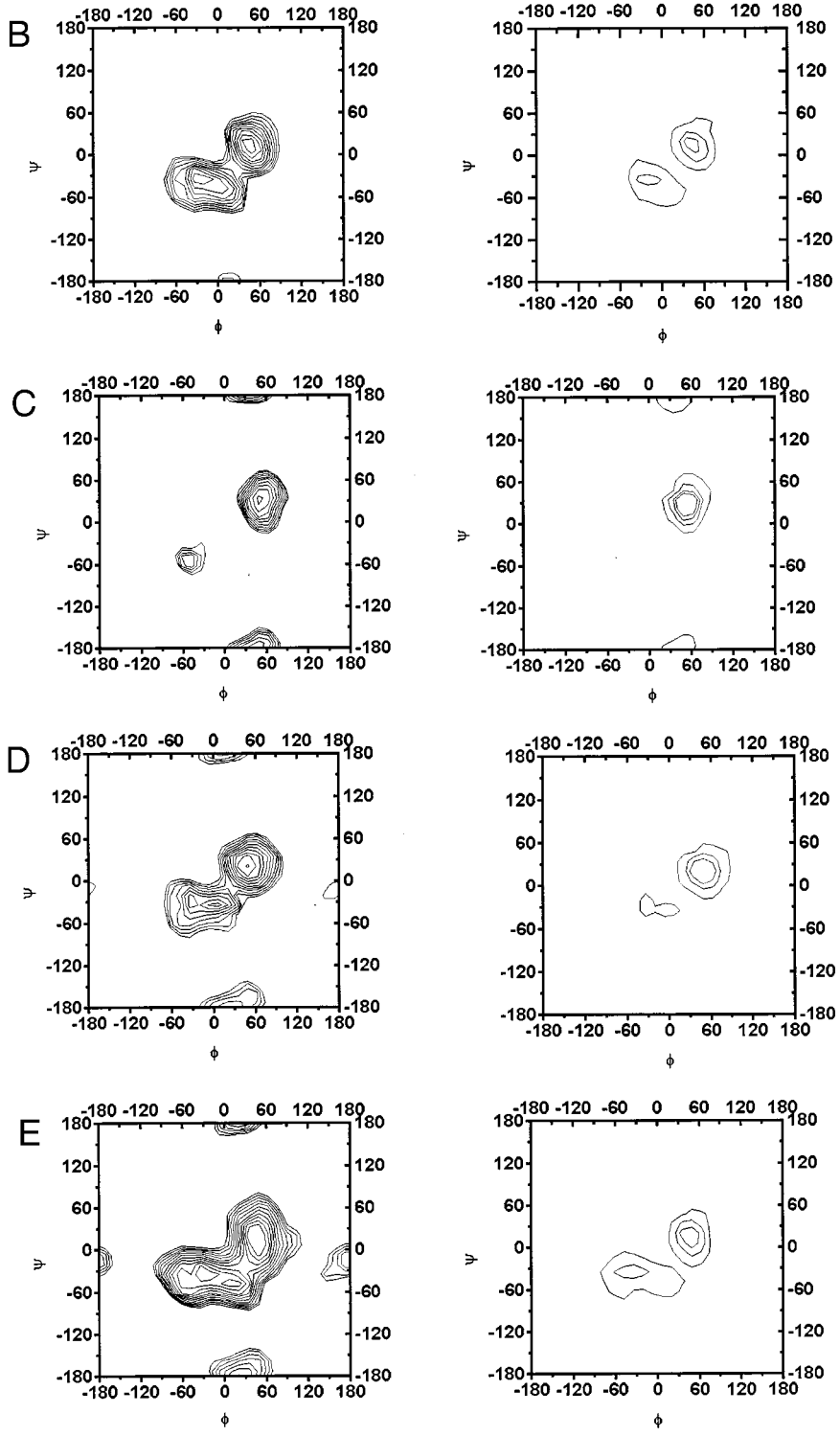

Figure 2. *(Continued)*

Additional information on the conformational stability of the different minima was obtained from MD simulations with the MM3* force field using the continuum GB/SA (Generalized Born solvent-accesible Surface Area) solvent model for water.[16] Independently from the starting minimum, the calculated trajectories showed several interconversions among the three different regions, therefore presenting a clear resemblence to the adiabatic surface described above.

The presence of the same minima, although with different populations was predicted from molecular mechanics calculations for the other analogues **2** and **3** (see Table 1

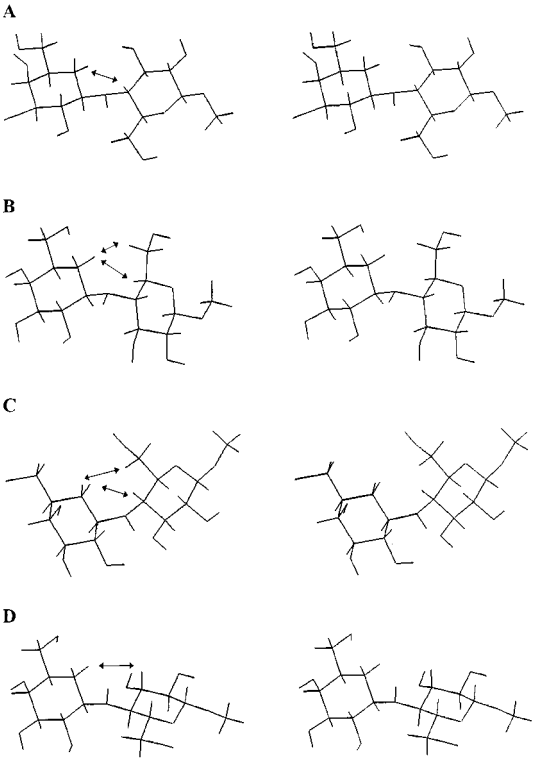

Figure 3. Stereoscopic views of the low-energy conformations obtained by MM3* calculations for compound **3**-$NH_{(proR)}$; from top to bottom: (A) *syn*-Φ/*syn*-Ψ (*exo*-anomeric), (B) *syn*-Φ/*anti*-Ψ, (C) *anti*-Φ/*syn*-Ψ, (D) non-*exo*-anomeric; key distances involving H-7 equatorial (H7-e) and axial (H-7a) protons are also given for the four conformers; basically, the shapes of every conformer are similar for compounds **2** and **3**.

and Figure 3). For carbalactose **2,** the map is similar to that reported for the natural analogue **4**, with an important contribution of the *syn*-Φ/*syn*-Ψ conformer, although with the presence of a fourth conformer, located at Φ/Ψ = −60/0, that is, with a non-*exo*-anomeric orientation (non-*exo*/*syn*-Ψ). Three different maps were calculated for compound **3**, with a nitrogen atom at the interglycosidic position. The first one, corresponding to an NH_2 group (**3**$^{\#1}$), considers the conformational behaviour at acidic pH. Two more maps were calculated with NH at the bridge, but with different relative orientations (pro*S*, pro*R*) of the proton at the nitrogen (**3**$^{\#2}$ and **3**$^{\#3}$). It can be observed that for the NH_2 and NH_{proS} derivatives, the maps are fairly similar with more than 80% of the *syn*-Φ/*syn*-Ψ conformer. Minor contributions of the non *exo* and *anti*-Ψ forms may be appreciated (<15%). The map for the virtual NH_{proR} derivative would predict a higher percentage of the non-*exo* form (50%). Since the steric energy values provided by MM3* for both NH_{proS} and NH_{proR} derivatives are fairly similar, the final expectations for **3** at high pH should correspond to 66% of *syn*-Φ/*syn*-Ψ, 32% non-*exo*-Φ/*syn*-Ψ, and 2% *syn*-Φ/*anti*-Ψ conformers.

NMR Spectroscopic Studies

The validity of the theoretical results has been tested using NMR measurements, especially NOEs. The assignment of the resonances was made through a combination of COSY, HSQC, and TOCSY experiments at 500 MHz, recorded under a variety of temperatures to try to avoid signal overlapping. Second order analysis of the spectra and ^{1}H-coupled-HSQC was performed to obtain refined δ and *J* values. The results are shown in Table 2 **(1)**, Table 3 **(2)**and Table 4 **(3)**.

Table 2. ^{1}H and ^{13}C NMR chemical shifts (δ, ppm) and coupling constants (*J*, Hz) of compound **1** in D_2O

	δ (ppm)	*J* (Hz)
H1	4.86	4.2
H2	3.62	9.5
H3	3.77	11.0
H4	2.87	11.0
H5	3.92	2.0, 5.0
H6a	4.06	−12.0
H6b	3.98	
H1′	4.59	9.5
H2′	3.58	9.5
H3′	3.67	3.0
H4′	3.98	1.0
H5′	3.70	n.d.
H6a′	3.72	n.d.
H6b′	3.72	n.d.
OMe	3.41	

Table 3. ^{1}H and ^{13}C NMR chemical shifts (δ, ppm) and coupling constants (*J*, Hz) of compound **2** in D_2O at pH 7.0

	δ (ppm)	*J* (Hz)		δ (ppm)
H1	4.75	7.7	C1	195
H2	3.20	8.1	C2	78
H3	3.4−3.5	n.d.	C3	−
H4	3.4−3.5	n.d.	C4	−
H5	3.4−3.5	<1, 2.8	C5	−
H6a	4.02	−12.4	C6a	67
H6b	3.91		C6b	66
H1′	3.4−3.5	−	C1′	−
H2′	3.4−3.5	9.5	C2′	−
H3′	3.43	2.0	C3′	−
H4′	3.94	1.0	C4′	75
H5′	1.65	5.1, 9.5	C5′	45
H6a′	3.61	−11.5	c6a′	68
H6b′	3.52		C6b′	68
H7e	1.95	3.6	C7e	35
H7a	1.25	−12.5	C7a	35
OMe	3.44		OMe	63.5

The key conformational information was obtained from NOE experiments. 2D-NOESY,[17] 2D-ROESY and 1D-DPFGSE NOESY[18] spectra were acquired. Our analysis was performed on the basis of the exclusive[19] interresidue NOEs that unequivocally characterize the *syn*-Φ/*syn*-Ψ, *syn*-Φ/*anti*-Ψ, and *anti*-Φ/*syn*-Ψ regions of the conformational map. For β(1→4) disaccharides such as **1**−**4**, these are H1′−H4 and H1′−H6sr (*syn*-Φ/*syn*-Ψ), H1′−H3 (*syn*-Φ/*anti*-Ψ), and H4−H2′ (*anti*-Φ/*syn*-Ψ), respectively. Additional NOES appear for carbasugars involving the equatorial (H-7e) and axial (H-7a) protons. For these compounds **2** and **3**, one exclusive interresidue NOE is now available for the non-*exo*/*syn*-Ψ region, namely H7e−H3.

Table 4. ^{1}H and ^{13}C NMR chemical shifts (δ, ppm) and coupling constants (*J*, Hz) of compound **3** in D_2O at pH 4.9 and 7.7

pH 4.9	δ (ppm)	*J* (Hz)		δ (ppm)	*J* (Hz)	pH 7.7	δ (ppm)	*J* (Hz)		δ (ppm)	*J* (Hz)
H1	4.41	8.0	C1	106.4	166.3	H1	4.35	7.9	C1	106.0	165.1
H2	3.35	8.7	C2	78.8	146.6	H2	3.26	8.6	C2	76.0	146.6
H3	3.71	9.8	C3	77.1	142.9	H3	3.4	9.2	C3	77.4	135.5
H4	3.30	10.3	C4	60.1	146.6	H4	2.62	9.7	C4	60.2	135.5
H5	3.38	m, 4	C5	75.4	131.8	H5	3.45	2.5, 5.7	C5	79.6	141.0
H6a	4.01	−12.3	C6a	62.5	142.9	H6a	4.02	−12.3	C6a	63.6	144.8
H6b	3.85		C6b	62.5	144.8	H6b	3.8		C6b	63.6	144.8
H1′	3.20	m	C1′	63.9	148.5	H1′	2.55	m	C1′	61.4	128.1
H2′	3.82	10.0	C2′	73.4	144.8	H2′	3.45	−	C2′	76.5	144.8
H3′	3.51	9.7	C3′	74.7	141.0	H3′	3.45	−	C3′	77.4	141.0
H4′	4.08	<1	C4′	71.6	148.5	H4′	4.05	<1	C4′	72.0	148.5
H5′	1.84	m	C5′	41.6	133.6	H5′	1.75	1, 3.4, 8	C5′	41.3	118.8
H6a′	3.71	−10.3	c6a′	64.6	142.9	H6a′	3.63	6.4	C6a′	64.8	142.9
H6b′	3.55	m	C6b′	64.6	150.3	H6b′	3.53	−11.0	C6b′	64.8	144.8
H7e	2.10	3.3	C7e	26.3	129.9	H7e	1.88	<1	C7e	29.8	129.9
H7a	1.50	−12.6	C7a	26.3	114.2	H7a	1.15	3.4	C7a	29.8	126.3
OMe	3.55		OMe	59.9	144.8	OMe	3.58		OMe	59.9	144.8

In addition, the presence of H7e−H4, H7e−H5, and H7a−H4 NOEs could help to further characterize the *syn*-Φ/*syn*-Ψ, *syn*-Φ/*anti*-Ψ, and *anti*-Φ/*syn*-Ψ regions, respectively.

The relevant experimental inter-residue proton−proton distances are shown in Table 5. Due to severe overlapping of the key protons, no unambiguous experimental information could be extracted for compound **2**. The data in Table 5 indicate that, for **1**, it is not possible to justify simultaneously all the observed NOEs with just one conformer. At least qualitatively, the presence of strong NOEs between H1′ and H3 indicate that the global minimum *syn*-Φ/*anti*-Ψ is heavily populated in solution. The NOE between H1′ and H4 has half the intensity of the previous one and indicates the presence of the *syn*-Φ/*syn*-Ψ conformer. This is conformed by the NOEs between H1′ and both $H6_{pro R,S}$, since these contacts are exclusive for this minimum. Finally, the existence of the *anti*-Φ/*syn*-Ψ conformer is also confirmed by the NMR spectroscopic data. The existence of the H2′/H4 NOE can only be explained by the occurrence of this geometry in solution. From a quantitative point of view, the distances obtained from the molecular mechanics distributions were compared with those estimated experimentally, by using a full relaxation matrix approach.[17] It can be observed that the agreement is satisfactory, and that the population of **1** can be explained with a 55:30:15 conformational distribution among the three mentioned minima. Nevertheless, it should be noted that, according to Neuhaus and Williamson "*...the ability to fit NOE data using predicted conformations cannot be taken to mean that those conformations are necessarily those that are present; other choices might well fit the NOE data also.*"[17]

The NMR experimental data for **3** were recorded at two different pH values, namely 7.7 and 4.9 units, which should correspond to the presence of neutral NH and protonated NH_2 groups. Despite some chemical shift differences (Table 4), the observed key inter-residue NOEs were basically identical, with very strong H1′−H4, H7e−H4, and H1′−$H6_{pro R,S}$ NOEs. These NOEs, as mentioned above, show the major existence of conformer *syn*-Φ/*syn*-Ψ. A very minor participation of the *syn*-Φ/*anti*-Ψ conformer could be inferred at acid pH, since the H1′−H3 and H7e−H5 NOEs could be detected at the noise intensity level. The absence of the H2′−H4 and H7a−H4 NOEs indicates that the presence of the *anti*-Φ/*syn*-Ψ conformer is below experimental detection. Again, at acidic pH, an almost quantitat-

Table 5. Relevant interresidue and ensemble average $<r^{-6}>^{-1/6}$ proton-proton distances (Å); strong, medium, and weak experimental NOEs are denoted by s, m, and w; short distances which would produce observable NOEs are marked in bold

Proton pair	Expected distances for conformer (Å)				Ensemble average expected/*observed distances from NOEs* (Å)				Experimental NOE intensities		
	A	B	C	D	**1**	**2**	**3**$^{\#1[a]}$	**4**$^{[13]}$	**1**	**3**	**4**$^{[13]}$
H1′−H4	**2.5**	3.6	3.7	**2.3**	3.1/*3.3*[b]	2.5/ ov[b]	2.7/*2.6*[b]	2.4/*2.4*[b]	m	ms,ms[c]	s
H1′−H3	4.6	**2.1**	4.5	3.7	2.9/2.8	3.5/ ov[b]	3.4/3.6	3.3/3.1	s	nd, vw	w
H1′−H6s	**2.2**	3.8	3.8	4.2	3.2/3.6	3.4/ ov[b]	3.1/3.5	2.5/3.0	w	w	mw
H1′−H6r	**2.7**	4.8	5.5	4.7	3.9/3.6	3.0/ ov[b]	3.2/3.5	3.3/3.0	w	w	mw
H7a−H4	3.3	4.4	**2.2**	4.7	na	na/ov	3.5/>3.6	na	na	nd, nd	na
H7e−H4	**2.2**	4.1	3.3	3.9	na	na/ov	2.4/2.5	na	na	ms, s	na
H7e−H5	5.0	2.3	4.3	4.7	na	na/ov	4.6/>3.6	na	na	nd, nd	na
H7e−H3	4.3	4.1	5.2	**2.9**	na	na/ov	4.2/>3.6	na	na	nd, nd	na
H7e−H6a	4.5	**2.3**	**2.4**	5.3	na	na/ov	4.1/>3.6	na	na	nd, nd	na
H2′−H4	4.5	4.6	**2.5**	4.2	*3.4/3.3*	3.7/ov	4.5>3.6	3.6/>3.6	mw	nd, nd	nd

[a] The predicted NOEs and distances results for **3**$^{\#1}$ and **3**$^{\#2}$ are similar. Those for **3**$^{\#3}$are similar to those predicted for **2**. − [b] Experimental derived distances are italized. Estimated error is 15% Maximum observable distance is estimated to be 3.6 Å. − [c] 'Two experimental intensity values are given for **3**, corresponding to acidic and basic pH. na, not applicable. ov, overlapping.

ive agreement between the experimental NOEs and those values obtained from the population distribution using a full-relaxation matrix approach was obtained. The *syn*-Φ/*anti*-Ψ population at every pH should be probably slightly smaller than the predicted 10%, and the populations of this pseudodisaccharide can be explained with a 95:5 conformational distribution between the *syn*-Φ/*syn*-Ψ and the *syn*-Φ/*anti*-Ψ regions. Regarding the presence of the non-*exo* conformers at high pH, although the molecular mechanics map for **3** predicted some participation of this minimum, the lack of its key H7e−H3 NOE, together with the high intensity values observed for the three key NOEs corresponding to the *syn*-Φ/*syn*-Ψ conformer, indicates that its population in solution should be smaller than that which can be experimentally detected (<5%). Regarding compound **2,** for which only the *syn*-*exo*-anomeric and non-*exo*anomeric conformations are predicted by the MM3* calculations, no unambiguous experimental evidences could be obtained. However, since the only difference with compound **3** resides at the interglycosidic position, no major conformational differences are to be expected with respect to those of compound **3**.

In conclusion, all the molecular mechanics and NMR results have allowed us to demonstrate the different conformational behaviour of *S*-lactose with respect to its *O*-analogues. Summarising, the global minima of **1** adopt *exo-anomeric* conformations around Φ, but the orientations around the aglyconic bond Ψ are rather different between *S*- and *O*-glycosyl compounds. The major conformer for *O*-glycosides is always centred at the *syn*-Ψ region. However, for *S*-lactose **1**, the *anti* conformer is predominant. It is also noteworthy to emphasize the participation of *anti*-Φ conformers for **1**, with a torsional variation of 120° of the Φ angle, which is very unusual for β-*O*-glycosides.[20] Therefore, *S*-glycosides may also display significant conformational variations around the Ψ angle as is also observed for β-*C*-lactosides.[6,14,15] Similar results have also been observed for other *S*-glycosides with different stereochemistries at their glycosidic linkages.[9] The variations in bond lengths and angles may provide the answer to the much higher flexibility of **1** versus its natural *O*-analogue. The conformation around Φ seems to be similar in all compounds **1**−**4**. For **1**, a limited stereoelectronic stabilization provided by the *exo-anomeric* effect should be expected.[8] Moreover, for **2** and **3**, with no acetal-type moiety, this stereoelectronic stabilization is no longer possible. Therefore, the explanation for the preference should mainly reside in steric effects, probably 1,3-type interactions. In fact, for the regular $^4C_1$(D) chairs, there is a 1,3-type interaction between one equatorially substituted *C*-2 (gluco and galacto-series, as in **1**−**4**) and the aglycon when the non-*exo*-anomeric (*non-exo*) conformation is considered (Figure 3). There are no such steric interactions for the *exo*-anomeric (*exo*) and the *anti* conformations. Therefore, this interaction is probably the origin of the strong preference of the *exo*-anomeric orientation in **1**−**3**. For *O*-glycosides, such as **4**, it is obvious that the stereoelectronic effect will be additionally superimposed, with a subsequent further stabilization of the *exo*-anomeric orientation, thus providing the explanation for the basically unique conformation around Φ angle of natural oligosacharides.

According to the calculations for **2** and **3**, for which similar bond lengths and angles to **4** occur, the force field calculations[12] suggest that in the absence of stereoelectronic stabilisation, conformations which are not consistent with the *exo-anomeric* disposition could be adopted (between 4−50%), which obviously will depend on the strength of the above mentioned 1,3-type interaction. That the presence of non-exoanomeric conformers could not be experimentally proven, suggest that this 1,3-type interaction is slightly underestimated in the MM3* programme.

Biological Activity

Compounds **1**−**3** were tested as *E. coli* β-galactosidase inhibitors.[21] Thiolactoside **1** was shown to be a moderate inhibitor with a K_I of 7.7 mM, assuming a competitive inhibitor model. The carbasugars **2** and **3** did not inhibit *E. coli* β-galactosidase up to 10 mM concentration. A model for the binding of C-lactose to this enzyme was recently proposed by us.[6] The proposed model implicated galactose O-5 in key interactions with Asn-102, Tyr-503 and His 540. The lack of inhibition of the carbalactosides indicate that indeed O-5 plays a determinant role in the binding process between the sugar and the enzyme. On the other hand, the enzyme accepts *C*- and *S*-glycosyl compounds in the binding site and both of them show similar inhibition abilities.

Conclusions

The results presented herein clearly show that the flexibility around the glycosidic linkages of pseudoglycosides may be determined by NMR experiments in combination with molecular mechanics calculations. In addition, the conformational changes observed, especially for *S*-glycosides, also reflect the small energy barriers between the different energy regions. Thus, conformations different from the major one existing in solution may be bound by the binding site of proteins without major energy conflicts. These results, along with those previously obtained by us for C-glycosides,[6,14] are important for drug design. For the binding of a flexible compound to a protein, usually one of the existing conformations should be selected out of the ensemble.[22] Therefore, a negative binding entropy will be expected, thus decreasing the energy of binding.[23] Consequently, the flexibility of *S*-disaccharides may be a limitation in order to use them as therapeutic agents. Nevertheless, these compounds may be excellent probes to study the combining sites of proteins and enzymes.[5,6] Along with carbadisaccharides, which have been shown to act as good acceptors of fucosyl transferases,[24] they may also serve as test compounds to compare conformational properties of oligosaccharides.

Experimental Section

Materials: Buffer salts, β-galactosidase from *E. coli* and *O*-nitrophenyl-β-D-galactopyranoside were from commercial sources (Sigma-Aldrich).

Methyl 4*S*-(β-DGalactopyranosyl)-4-thio-α-D-glucopyranoside (Methyl α-Thiolactoside, 1): Compound **1** was obtained from methyl 2,6-*O*-acetyl-4-*S*-(2, 3, 4, 6-tetra-*O*-acetyl-β-D-galactopyranosyl)-3-*O*-sulfo-4-thio-α-D-glucopyranoside caesium salt[25a] (**5**) after hydrolysis of the sulfate group and deacetylation. In particular, 30 μL of a solution of THF/H_2SO_4/H_2O (30:0.3:0.11) was added to a solution of **5** (5 mg, 6μmol) in 60 μL of THF, and stirred at room temperature for 30 minutes. The reaction mixture was then diluted with ethyl acetate, washed with sodium bicarbonate, dried with sodium sulfate, and concentrated to dryness. Flash chromatography of the residue (silica, chloroform/methanol 10:1) afforded the corresponding desulfated compound (2 mg, 54%). This product was treated with 0.3 M sodium methoxide in methanol for 15 minutes at room temperature and neutralized with Amberlite IR-120 resin. Solvent evaporation and flash chromatography of the residue (silica, chloroform/methanol 10:1) yielded pure **1** (1 mg, 84%) with the same physical data as described previously for methyl 4-*S*-(β-D-galactopyranosyl)-4-thio-α-D-glucopyranoside (**1**).[25b] The synthesis of compounds **2** and **3** has been published elsewhere.[3,24]

Molecular Mechanics and Dynamics Calculations: Molecular mechanics and dynamics calculations were performed using the MM2* , MM3*, and AMBER* force fields as implemented in MACROMODEL 4.5.[12] Φ is defined as H1′−C1′−Y−C4 and Ψ as C1′−Y−C4−H4. Thus, the atoms of the nonreducing end are primed. Only the *gg* and *gt* orientations of the lateral chain were used for the Glc moieties, and the *tg* and *gt* orientations were used for the Gal residues. Separate calculations for a dielectric constant ε = 80 and for the continuum GB/SA solvent model were performed. First, potential energy maps were calculated for the pseudodisaccharides: relaxed (Φ,Ψ) potential energy maps were calculated as described. [13,26] Four initial geometries were considered: *cc*, *cr*, *rr* and *rc*, obtained by combining the positions *r* (reverse clockwise) and *c* (clockwise) for the orientation of the secondary hydroxyl groups of both pyranoid moieties. The first character corresponds to the nonreducing moiety, and the second one to the reducing one. In total, 32 maps were calculated for **1**−**2** and 48 for **3**. The previous step involved the generation of the corresponding rigid-residue maps by using a grid step of 18°. Then, every Φ,Ψ point of this map was optimised using 200 steepest-descent steps, followed by 1000 conjugate gradient iterations. From these relaxed maps, adiabatic surfaces were built, and the probability distributions calculated for each ϕ, ψ point according to a Boltzmann function at 303 K.

The energy minima structures (see text) were used as the starting geometry for molecular dynamics (MD) simulations[27] at 300 K, with the GB/SA solvent model, and a time step of 1 fs. The equilibration period was 100 ps. After this period, structures were saved every 0.5 ps. The total simulation time was 1 ns for every run. Average distances between intra-residue and inter-residue proton pairs were calculated from the dynamics simulations.

NMR Spectroscopy: NMR experiments were recorded with a Varian Unity 500 spectrometer with an approximately 2 mg/mL solution of the pseudodisaccharides at different temperatures. Chemical shifts are reported in ppm, using external TMS (0 ppm) as reference. The double quantum filtered COSY spectrum was performed with a data matrix of 256 × 1 K to digitize a spectral width of 2000 Hz. 16 scans were used with a relaxation delay of 1 s. The 2D TOCSY experiment was performed using a data matrix of 256 × 2 K to digitize a spectral width of 2000 Hz. Four scans were used per increment with a relaxation delay of 2 s. MLEV 17 was used for the 100 ms isotropic mixing time. The one-bond proton-carbon correlation experiment was collected in the ^{1}H-detection mode using the HSQC sequence and a reverse probe. A data matrix of 256 × 2K was used to digitize a spectral width of 2000 Hz in F_2 and 10000 Hz in F_1. Four scans were used per increment with a relaxation delay of 1 s and a delay corresponding to a *J* value of 145 Hz. A BIRD pulse was used to minimize the proton signals bonded to ^{12}C. ^{13}C decoupling was achieved by the WALTZ scheme.

NOESY experiments were performed with the selective 1D double-pulse field-gradient spin-echo module,[18] using four different mixing times: 150, 300, 450, and 600 ms. 2D NOESY, 2D-ROESY, and 2D-T-ROESY[28] experiments were also performed with the same mixing times, and using 256 × 2 K matrices. The experiments for **3** were repeated at two different pHs.

NOE Calculations: NOESY spectra were simulated according to a complete relaxation matrix approach, following the protocol previously described,[13,26] using four different mixing times (between 150 and 600 ms). The spectra were simulated from the average distances $<r^{-6}>_{kl}$ calculated from the relaxed energy maps at 303 K. Isotropic motion and external relaxation of 0.1 s^{-1} were assumed. A τ_c of 95 ps was used to obtained the best match between experimental and calculated NOEs for the intra-residue proton pairs (H1′/H3′, H1′/H5′, and/or H1/H3).

All the NOE calculations were automatically performed by a home-made program, available from the authors upon request.[13]

Enzyme Inhibition Measurements: The enzymatic activity of β-galactosidase from *E. coli* was followed using *O*-nitrophenyl-β-D-galactopyranoside as substrate and measuring the released *O*-nitrophenol by HPLC. The enzyme (0.3 μg/mL) was incubated with the substrate (0.5 mM) in 20 μL of buffer (sodium phosphate 50 mM, pH 7, $MgCl_2$ 1 mM, β-mercaptoethanol 5 mM) and in the presence of several concentrations (from 0 to 20 mM) of compounds **1**, **2**, or **3**. After 4 min incubation at 310 K, the samples were diluted with 200 μL of cold HPLC eluent (water/acetonitrile/trifluoroacetic acid, 65:35:0.1), and injected into the HPLC system (reverse phase C-18 column, UV detection at 275 nm). The corresponding inhibition constants K_i were calculated assuming a competitive inhibition model.

Acknowledgments

Financial support by DGICYT (Grant PB96−0833) is gratefully acknowledged. J. L. A. thanks CAM and MEC for fellowships. A. G. thanks Gobierno Vasco for a fellowship. S. O. thanks Y. Kajihara (Yokohama City University, Japan) for purification of compounds **2** and **3**.

[1] [1a] H. J. Gabius, S. Gabius, *Glycosciences: Status and Perspectives*, Chapman & Hall, London, **1997**. − [1b] *Chemistry of C-glycosides* (Eds.: W. Levy, D. Chang), Elsevier: Cambridge, **1995**. − [1c] *C-Glycoside synthesis*, M. D. H. Postema, CRC Press, Boca Raton, **1995**. − [1d] H. Driguez, *Topics Curr. Chem.* **1997**, *187*, 85−116. − [1e] J. S. Andrews, B. M. Pinto, *Carbohydr. Res.* **1995**, *270*, 51−62. − [1f] H. Yuasa, H. Hashimoto, *Reviews on Heteroatom Chemistry*, **1999**, *19*, 35−65.

[2] [2a] B. A. Johns, Y. T. Pan, A. D. Elbein, C. R. Johnson, *J. Am. Chem. Soc.* **1997**, *119*, 4856−4865. − [2b] Special volume on

glycosciences (Eds.: H.-J. Gabius, F. Sinowatz), *Acta Anat*. **1998,** *161,* 1−276.
[3] S. Ogawa, K. Hirai, T. Odagiri, N. Matsunaga, T. Yamazaki, A. Nakajima, *Eur. J. Org. Chem.* **1998**, *1,* 1099−1109, and references therein.
[4] M. S. Searle, D. H. Williams, *J. Am. Chem. Soc.* **1992,** *114*, 10690−10697.
[5] E. Montero, M. Vallmitjana, J. A. Perez-Pons, E. Querol, J. Jiménez-Barbero, J. Cañada, *Febs Lett* **1998**, *421*, 243−248.
[6] J. F. Espinosa, E. Montero, A. Vian, J. L. Garcia, H. Dietrich, M. Martín-Lomas, R. R. Schmidt, A. Imberty, F. J. Cañada, J. Jiménez-Barbero, *J. Am. Chem. Soc.* **1998**, *120*, 10862−10871.
[7] A general survey of conformation of carbohydrates and analogues is presented in: A. D. French, J. W. Brady, *Computer Modelling of Carbohydrate Molecules*, American Chemical Society, **1990**.
[8] [8a] R. U. Lemieux, S. Koto, D. Voisin, *Am. Chem. Soc., Symp. Ser*. **1979,** *87*, 17−29. − [8b] G. R. J. Thatcher, *The Anomeric Effect and Associated Stereoelectronic Effects*; American Chemical Society: Washington, DC, **1993**. − [8c] I. Tvaroska, T. Bleha, *Adv. Carbohydr. Chem. Biochem.* **1989**, *47*, 45−103. − [8d] A. J. Kirby, *The Anomeric Effect and Related Stereoelectronic Effects at Oxygen*, Springer-Verlag, Heidelberg, Germany, **1983**.
[9] [9a] K. Bock, J. O. Duus, S. Refn, *Carbohydr. Res.* **1994**, *253*, 51−67. − [9b] A. Geyer, G. Hummel, T. Eisele, S. Reinhardt, R. R. Schmidt, *Chem. Eur. J.* **1996**, *2*, 981−988. − [9c] U. Nilsson, R. Johansson, G. Magnusson, *Chem. Eur. J.* **1996**, *2*, 295−302. − [9d] B. Aguilera, J. Jiménez-Barbero, A. Fernandez-Mayoralas, *Carbohydr. Res.* **1998**, *308*, 19−27.− [9e] E. Raimbaud, A. Buleon, S. Perez, *Carbohydr. Res.* **1992**, *227*, 351−363.
[10] [10a] J. O. Duus, K. Bock, S. Ogawa, *Carbohydr. Res.* **1994**, *252*, 1−18. − [10b] J. O. Duus, J. F. Guzmán, K. Bock, S. Ogawa, F. Yokoi, *Carbohydr. Res.,* **1991**, *209*, 51−65. − [10c] K. Bock, J. F. Guzman, S. Ogawa, *Carbohydr. Res.* **1988**, *174*, 354−359. − [10d] K. Bock, S. Ogawa, M. Orihara, *Carbohydr. Res.* **1989**, *191*, 357−363.
[11] For a detailed description of conformational analysis of carbohydrates using NMR and calculations, see: [11a] T. Peters, B. M. Pinto, *Curr. Opin. Struct. Biol*. **1996**, *6*, 710−720. − [11b] A. Imberty, *Curr. Opin. Struct. Biol*. **1997**, *7*, 617−623. − [11c] J. Jiménez-Barbero, J. L. Asensio, J. Cañada, A. Poveda, *Curr. Opin. Struct. Biol*. **1999**, *9*, 549−555.
[12] F. Mohamadi, N. G. J. Richards, W. C. Guida, R. Liskamp, C. Caufield, G. Chang, T. Hendrickson, W. C. Still, *J. Comput. Chem.* **1990**, *11*, 440−467. The MM3* force field (N. L. Allinger, Y. H. Yuh, J. H., Lii, *J. Am. Chem. Soc.* **1989**, *111*, 8551−8558) implemented in MACROMODEL differs of the regular MM3 force field in the treatment of the electrostatic term since it uses charge-charge instead of dipole-dipole interactions. The AMBER* force field used in this work is parametrised for sugars, S. W. Homans, *Biochemistry,* **1990**, *29,* 9110.
[13] J. L. Asensio, J. Jiménez-Barbero, *Biopolymers* **1995**, *35*, 55−73.
[14] [14a] J. F. Espinosa, M. Martín-Pastor, J. L. Asensio, H. Dietrich, M. Martín-Lomas, R. R. Schmidt, J. Jiménez-Barbero, *Tetrahedron Lett.* **1995**, *36*, 6329−6332. − [14b] J. F. Espinosa, F. J. Cañada, J. L. Asensio, M. Martín-Pastor, H. Dietrich, M. Martín-Lomas, R. R. Schmidt, J. Jiménez-Barbero, *J. Am. Chem. Soc.* **1996**, *118*, 10862−10871.
[15] [15a] J. F. Espinosa, H. Dietrich, M. Martín-Lomas, R. R. Schmidt, J. Jiménez-Barbero, *Tetrahedron Lett.* **1996**, *37*, 1467−1470. − [15b] J. F. Espinosa, F. J. Cañada, J. L. Asensio, H. Dietrich, M. Martín-Lomas, R. R. Schmidt, J. Jiménez-Barbero, *Angew. Chem.* **1996**, *Int. Ed. Engl* 35, 303−306. − [15c] M. Martín-Pastor, J. F. Espinosa, J. L. Asensio, J. Jiménez-Barbero, *Carbohydr. Res.* **1997**, *298*, 15−47.
[16] W. C. Still, A. Tempczyk, R. C. Hawley, T. Hendrickson, *J. Am. Chem. Soc.* **1990**, *112*, 6127−6128.
[17] D. Neuhaus, M. P. Williamson, *The Nuclear Overhauser Effect in Structural and Conformational Analysis,* VCH Publishers, New York, **1989**.
[18] K. Stott, J. Stonehouse, J. Keeler, T.-L. Hwang, A. J. Shaka, *J. Am. Chem. Soc***. 1995**, *117*, 4199.
[19] J. Dabrowski, T. Kozar, H. Grosskurth, N. E. Nifant'ev, *J. Am. Chem. Soc.* **1995,** *117*, 5534.
[20] C. Landersjo, R. Stenutz, G. Widmalm, *J. Am. Chem. Soc.* **1997**, *119*, 8695−8701.
[21] J. L. Asensio, F. J. Cañada, A. García, M. T. Murillo, A. Fernández-Mayoralas, B. A. Johns, J. Kozak, Z. Zhu, C. R. Johnson, J. Jiménez-Barbero, *J. Am. Chem. Soc.* **1999**, *121*, 11318−11331.
[22] For a recent review on glycosidases, see: A. T. Vasella, T. D. Heightman, *Angew. Chem. Int. Ed. Engl.* **1999**,*38*, 750.
[23] For conformational selection in carbohydrate recognition by proteins, besides ref.[11] see: [23a] M. Gilleron, H.-C. Siebert, H. Kaltner, C. W. von der Lieth, T. Kozar, K. M. Halkes, E. Y. Korchagina, N. V. Bovin, H.-J. Gabius, J. F. G. Vliegenthart, *Eur. J. Biochem.* **1998,** *249*, 27−38. − [23b] A. Poveda, J. Jiménez-Barbero, *Chem. Soc. Rev.* **1998**, *27,* 133−143. − [23c] J. L. Asensio, J. F.Espinosa, H. Dietrich, F. J. Cañada, R. R. Schmidt, M. Martín-Lomas, S. André, H. J. Gabius, J. Jiménez-Barbero, *J. Am. Chem. Soc.* **1999,** *121*, 8995−9000. For different implications of conformational restriction of the ligand upon protein binding, see: − [23d] D. R. Bundle, R. Alibés, S. Nilar, A. Otter, M. Warwas, P. Zhang, *J. Am. Chem***. *Soc.* **1998,** *120*, 5317−531. − [23e] N. Navarre, N. Amiot, A. H. van Oijen, A. Imberty, A. Poveda, J. Jiménez-Barbero, A. Cooper, M. A. Nutley, G. J. Boons, *Chem. Eur. J.* **1999**, *5*, 2281−2294.
[24] S. Ogawa, N. Matsunaga, H. Li, M. M. Palcic, *Eur. J. Org. Chem*. **1999**, 631−642.
[25] [25a] J. A. Calvo-Aín, F. G. Calvo-Flores, J. M. Expósito-López, F. Hernández-Mateo, J. J. García-López, J. Isac-García, F. Santoyo-González, A. Vargas-Berenguel, *J. Chem. Soc. Perkin Trans. 1.* **1997**, 1079−1081. − [25b] L. A. Reed, L. Goodman, *Carbohydr. Res.* **1981**, *94*, 91−99.
[26] J. F. Espinosa, M. Bruix, O. Jarreton, T. Skrydstrup, J.-M. Beau, J. Jiménez-Barbero, *Chem. Eur. J.* **1999**, *5*, 442−448.
[27] For a detailed description of conformational analysis of carbohydrates using MD simulations, see, R. J. Woods, *Curr. Opin. Struct. Biol*. **1995**, *5*, 591−598.
[28] T.-L. Hwang, A. J. Shaka, *J. Am. Chem. Soc***. 1992**, *114*, 3157.

Received October 18, 1999
[O99592]